General Disclaimer

One or more of the Following Statements may affect this Document

- This document has been reproduced from the best copy furnished by the organizational source. It is being released in the interest of making available as much information as possible.

- This document may contain data, which exceeds the sheet parameters. It was furnished in this condition by the organizational source and is the best copy available.

- This document may contain tone-on-tone or color graphs, charts and/or pictures, which have been reproduced in black and white.

- This document is paginated as submitted by the original source.

- Portions of this document are not fully legible due to the historical nature of some of the material. However, it is the best reproduction available from the original submission.

NASA TECHNICAL MEMORANDUM

NASA TM X-73658

NASA TM X-73658

THERMAL STRESS ANALYSIS OF A GRADED ZIRCONIA/METAL GAS PATH SEAL SYSTEM FOR AIRCRAFT GAS TURBINE ENGINES

by Christopher M. Taylor
Lewis Research Center
Cleveland, Ohio 44135

April 1977

1. Report No. NASA TM X-73658	2. Government Accession No.	3. Recipient's Catalog No.
4. Title and Subtitle THERMAL STRESS ANALYSIS OF A GRADED ZIRCONIA/METAL GAS PATH SEAL SYSTEM FOR AIRCRAFT GAS TURBINE ENGINES		5. Report Date 6. Performing Organization Code
7. Author(s) Christopher M. Taylor		8. Performing Organization Report No. E-9164 10. Work Unit No.
9. Performing Organization Name and Address National Aeronautics and Space Administration Lewis Research Center Cleveland, Ohio 44135		11. Contract or Grant No. 13. Type of Report and Period Covered Technical Memorandum
12. Sponsoring Agency Name and Address National Aeronautics and Space Administration Washington, D.C. 20546		14. Sponsoring Agency Code

15. Supplementary Notes

16. Abstract

A ceramic/metallic aircraft gas turbine outer gas path seal designed to enable improved engine performance is studied. Flexible numerical analysis schemes suitable for the determination of transient temperature profiles and thermal stress distributions in the seal are outlined. An estimation of the stresses to which a test seal is subjected during simulated engine deceleration from sea-level take-off to idle conditions is made. Experimental evidence has indicated that the surface layer of the seal is probably subjected to excessive tensile stresses during cyclic temperature loading. This assertion is supported by the analytical results presented. Brief consideration is given to means of mitigating this adverse stressing.

17. Key Words (Suggested by Author(s)) Stress analysis; Finite element method; Gas turbine engines; Seals; Cermets

18. Distribution Statement Unclassified - unlimited STAR Category 37

19. Security Classif. (of this report)	20. Security Classif. (of this page)	21. No. of Pages	22. Price*
Unclassified	Unclassified		

* For sale by the National Technical Information Service, Springfield, Virginia 22161

THERMAL STRESS ANALYSIS OF A GRADED ZIRCONIA/METAL GAS PATH SEAL SYSTEM FOR AIRCRAFT GAS TURBINE ENGINES

by Christopher M. Taylor*

Lewis Research Center

E-9164

SUMMARY

In order to improve aircraft gas turbine engine performance by raising turbine inlet temperatures to about 1811 K (2800° F), an improved high-pressure turbine outer gas path seal system is required. Current metallic seal systems are limited through material operating capability to temperatures of about 1366 K (2000° F).

One proposed form of improved seal is a plasma sprayed, layered zirconia/CoCrAlY system on a metallic substrate. Four ceramic or partially ceramic layers protect the substrate from the high temperatures of the hot turbine gases, the surface or top layer accommodating blade-seal ribs by virtue of its abradable nature. The present report outlines analyses to determine transient temperature and stress distributions on a seal and undertakes sample calculations.

During the normal operational cycle of an aircraft gas turbine engine the gas path seal will experience varying thermal stresses. Thermal cycling fatigue is therefore a concern. Indeed, experiments on a small version of the proposed engine seal have resulted in surface cracking during thermal fatigue testing. The calculations indicate that during a simulated engine deceleration cycle from sea-level take-off to idle conditions, the maximum seal temperature may occur below the seal surface. Such a temperature profile would promote tensile stresses in the surface layer. Finite-element analyses of the stress patterns developed show that tensile stresses exceeding the modulus of rupture could occur

---

*Lecturer in Mechanical Engineering, University of Leeds, Leeds, England; National Research Council - National Aeronautics and Space Administration Senior Research Associate at the Lewis Research Center in 1976-77.

in the top layer of the seal and hence the experimental evidence is corroborated. It is also demonstrated that stress analyses conducted using a two-dimensional finite element program are capable of predicting the same trends as those obtained with a more complicated three-dimensional analysis.

Two possible methods of introrucing a compressive stress into the surface layers of the seal at room temperature are investigated. This would result in reduced tensile stresses during operation and hence better thermal fatigue performance. Another possible way to improve the performance of the seal might be to alter the relative thickness of the layers which comprise it. A parametric study to investigate this is recommended and other aspects deserving attention in future studies are highlighted.

INTRODUCTION

A current trend in aircraft gas turbine practice is towards higher turbine inlet temperatures enabling an improved performance. The high-pressure turbine outer gas path seal system is an important feature as regards engine performance, since the greater the leakage across the blade tips the lower will be the turbine efficiency. Present day metallic seal systems are limited to temperatures of about 1366 K (2000^{o} F) and require cooling air to maintain them within material operating capabilities. This cooling air is bled from the compressor section and results in some lost performance as high-pressure air is removed from the cycle.

One proposed form of improved turbine outer gas path seal is a plasma sprayed, layered zirconia/CoCrAlY system on a metallic substrate (ref. 1). Such a seal is designed to have a temperature capability of about 1588 K (2400^{o} F) enabling projected turbine inlet temperatures of around 1811 K (2800^{o} F) to be accommodated. As well as allowing a reduction in the required cooling air, the proposed seal has a second important advantage in its abradable nature giving reduced rotor wear during blade and seal contacts. This abradibility should enable a tighter clearance to be maintained between the turbine first-stage blade tips and seal, hence improving the turbine efficiency.

There are a number of requirements to be met by the suggested seal system. These include satisfactory performance as regards oxidation and corrosion resistance, abradability, and hot gas and particulate erosion resistance, as well as the obvious need for structural integrity to be maintained. The

purpose of the present report is to investigate the structural integrity aspect. The study has involved finite element analyses of a seal to determine stress and distortion patterns likely to be encountered during steady-state and transient engine operating conditions. The analyses are intended to compliment experimental testing of the seal, which is somewhat smaller in size than will be required for full-scale engine use.

THE ENGINEERING PROBLEM

A cross section of the gas path seal studied is shown in figure 1. For the purpose of the current investigation the seal geometry was not varied. The composition of the layers of the seal is indicated on figure 1. The upper or top layer is comprised entirely of the ceramic zirconia, stabilized with yttria. It is the surface of this upper layer that is in contact with the hot turbine gases. Successive layers have a decreasing zirconia content - there being four layers in total sprayed onto the substrate material. Thus, a stepwise gradation of material composition is provided from fully ceramic at the gas path surface to a fully metallic substrate. The substrate has feet to locate the seal in guideways on the engine casing and is comprised of a cobalt based super alloy (Mar-M-509). A NiCrAl coat about 0.1 millimeter (0.004 in.) in thickness is used to improve the bonding of the ceramic system to the substrate, but this has not been considered in the analysis. The physical and mechanical properties of the materials of the seal are shown in table I. Many of these properties have been determined specifically in relation to the program of improved gas path sealing. These properties were used in the analyses performed, a linear variation being taken between the stated temperatures, and for reasonable extrapolations outside the ranges given. Where properties were unknown, reasoned guesses have been made.

During the operation of an aircraft gas turbine engine the outer gas path seal will experience varying temperature conditions. The possibility of fatigue due to cyclic thermal stressing must therefore be examined and an experimental program in this regard has been established. In the present work transient, as well as steady seal operating conditions, are considered. For the transient thermal analysis the temperatures of the hot turbine gases at the seal surface and cooling air fed from the compressor to the substrate back were simulated as shown in figure 2. The temperatures are representative of those in an engine

decelerated from sea-level take-off to idle conditions in a period of 1 minute, and have been estimated from seal surface and back face temperatures determined analytically (ref. 2).

The current work was seen as a first task stage, intended to investigate alternative analytical approaches and highlight areas worthy of future detailed study. To this end the following aspects have received attention.

(1) Transient thermal patterns in the seal have been determined, including a consideration of the effect of varying the heat-transfer coefficients at the seal surface and back face.

(2) Stress distributions throughout the seal during the assumed deceleration cycle conditions have been established. Computer programs employing both two- and three-dimensional finite elements have been used.

(3) Consideration has been given as to how the experimentally observed adverse stressing of the upper ceramic layer might be mitigated.

ANALYSIS

All computer programs used to generate the results presented in this report are available through the Computer Services Division of the National Aeronautics and Space Administration's Lewis Research Center, and were operated on the Center's UNIVAC 1100 computer.

Transient Thermal Analysis

The SINDA (Systems Improved Numerical Differencing Analyzer) program was used to generate transient temperature profiles throughout the seal during the deceleration cycle. The program enables analysis of thermal systems represented in electrical analogue, lumped parameter form. Axisymmetric thermal conditions were taken to apply. Indeed since the axial extremities of the seal were taken to be insulated (as no detailed information on thermal conditions there was available), the seal temperatures were effectively a function of only the radial coordinate.

Stress Analysis

Thermal stresses in the seal were estimated using two finite element programs, the one only capable of analyzing two-dimensional situations, the other having the capability of dealing with three-dimensional geometries. In this way it was hoped to learn how appropriate the use of the simpler two-dimensional analyses was in terms of being able to predict satisfactorily stresses in the seal.

The two-dimensional code employed was the FEATAGS (Finite Element Analysis, Temperature and General Stress) program. This code can deal with axisymmetric or plane bodies. The temperature data generated by the SINDA program was used as input to the two-dimensional stress code providing the thermal loading for the seal at specified time intervals during the engine deceleration cycle. The program can also undertake steady-state thermal analyses and was used to check the temperature patterns predicted by the SINDA code for the sea-level take-off steady-state conditions. Excellent agreement was found.

For three-dimensional stress analysis of the seal the MARC (Marc Analysis Research Corporation) program was employed. Since this program is in process of being established on the Lewis Research Center's UNIVAC computer, the transient thermal analysis capability it has was not employed. Rather the temperature profiles generated by the SINDA code (and taken to be a function of radius only) were used as the thermal loading input.

All analyses carried out with the stress codes assumed that the seal was free to distort as it required. That is, no boundary restrictions on its movement, even at the feet locating it to the engine casing, were applied. As will be seen the structural integrity of the seal is challenged even if it is allowed to expand freely. Computations have indicated that if the seal is restrained in any way the enhancement of the thermal stresses it sees are such as to suggest that material failure in some form would be inevitable.

All computations performed with the stress codes assumed that the materials of the seal behaved elastically even if stresses greater than those required for yielding or crack initiation were attained. However, both programs have a capability for dealing with plastic material behavior and an extension of the analysis of the seal incorporating such behavior might be appropriate in the future.

Distortions of the seal have also been determined but details will not be presented, since the ability of the seal to withstand the stresses to which it is subjected is the primary interest initially.

RESULTS AND DISCUSSION

Temperature Distributions

In determining the temperature profiles shown in figure 3 the following heat-transfer coefficients were employed at seal surface and back face, respectively: 5 700 and 11 400 $W/(m^2)(K)$ (1000 and 2000 $Btu/(hr)(ft^2)(^oF)$). The temperature distributions on the axial line of symmetry are shown. The analysis assumed axisymmetric conditions and as has been mentioned the axial variation of temperature at a fixed radius was small. Temperature profiles at sea-level take-off and idle (60 sec into the deceleration cycle but not quite steady state) conditions are shown, together with three profiles at 6, 12, and 20 seconds into the deceleration cycle.

It is immediately noticeable that during the transient variation of temperature between sea-level take-off and idle conditions, the situation may be obtained where the maximum seal temperature at any given time occurs below the seal surface. Such situations reflect the transference of heat from the seal surface to the turbine gases as the surface temperature of the seal exceeds that of the gases which has fallen rapidly. Despite the fact that the temperature of the seal at a time 12 seconds into the deceleration cycle is much less than at the steady-state sea-level take-off condition, the stressing of the seal may be more severe due to the temperature maximizing below the surface. For example, the possibility of subjecting the surface layer to undue tensile stresses becomes apparent. Figure 3 also illustrates well how the top four layers of the seal protect the substrate from high temperatures. The temperature drop across the substrate layer is very small due to its relatively high thermal conductivity.

The surface heat-transfer coefficients used in the determination of the temperature profiles shown in figure 3 are by no means precisely known parameters. The temperature profiles of figure 3 have, in the main, been used to determine seal stress distributions presented later. However, a brief examination of the effects of varying the heat-transfer coefficients, on both temperature and stress profiles, has been undertaken.

In figure 4 the temperature profiles A, C, and E of figure 3 are compared with profiles obtained using alternative heat-transfer coefficients. The heat-transfer coefficients already designated are termed case 1. For case 2 the heat-transfer coefficient at the seal surface was reduced by a factor of 10, the intention being to reflect a reduced heat-transfer capability possibly appropriate at the less turbulent gas flow conditions near engine idle. In addition, in case 3, it was assumed that the seal surfaces took up the temperature of the gases with which they were in contact.

It can be seen from figure 4 that the conditions of case 3 have only a minor effect on temperature distributions compared with case 1. However, reducing the heat-transfer coefficient by a factor of 10 at the hot surface has a noticeable, and expected, effect on the top surface temperatures at the sea-level take-off and idle conditions. Brief mention of the effect of such differences on the stress distributions will be made leter.

Stress Distributions

General remarks. - Before giving details of stresses developed in the seal it is necessary to clarify certain aspects of the finite element analyses and the manner in which the results are presented.

In the three-dimensional analysis, because of prevailing symmetry, it was only necessary to consider one quarter of the seal. As has been mentioned the temperatures in the seal were taken to be a function of radius only. The portion of the seal taken is shown, in figures 5 to 7, there being two views in order to present axial and circumferential stresses. The center lines of the views pass through the mid-point of the seal surface. It will be noted that the views are not scaled, the half length of the seal being, in fact, 3.5 times the half width and five times the de ' . In addition the curvature of the seal circumferentially has not been depicted although it was considered in the analysis.

Two forms of solution were effected in the two-dimensional analysis of the seal. Firstly, axisymmetric conditions were taken and, secondly, and alternatively, plane stress conditions were assumed axially. For the plane stress analyses curvature effects were neglected. A typical form of presentation of the calculated stresses is shown in figures 8 to 10. Data is given on central planes circumferentially and axially, although the results are for two-dimensional situations. In this way easy comparison with the three-dimensional analysis

results presented is possible, these being very nearly on central planes.

It is not proposed to describe here the details of the finite-element structures adopted to model the seal geometry. Neither will the precise spacial positions at which details of stresses are presented be given, since it is intended only to give an overall feel for magnitudes and their approximate location. In broad terms the stresses given are at points close to the interfaces concerned and close to the extremities of the sections considered. The positions at which stress values are given are similar for the two- and three-dimensional analyses.

It will be noted that only details of axial and circumferential stresses are presented. Radial and shear stresses are, in general, small in comparison, particularly in the interior of the seal. At the axial and circumferential extremities this is not always the case, but it is not proposed to mask major considerations by such details here. Since the radial and shear stresses are small it follows that the axial and circumferential stresses presented are very often effectively principal stresses. All the stress values are given in a Cartesian system constructed on the diagram center lines. This includes the stresses at the circumferential extremity of the three-dimensional seal geometry.

Results. - Details of the analytical results will now be presented and discussed. It should be explained that it has been assumed that the seal is in a stress-free state at ambient conditions, 294 K (70° F). In figures 5, 6, and 7 stress distributions corresponding, respectively, to the temperature distributions at sea-level take-off (A), 12 seconds into the deceleration cycle (C), and idle (E) of figure 3, are shown for the three-dimensional analysis. The moduli of rupture at the locations where stress results are presented are shown for the four ceramic layers.

The following major parts are worthy of note.

(1) At sea-level take-off steady-state conditions (fig. 5) the top layer of the seal is subjected to sizeable compressive stresses. The fourth layer, which is bonded to the substrate, is in considerable tension, the modulus of rupture having been exceeded in the elastic analysis. In fact, the material of the fourth layer would probably yield under these conditions, resulting in some stress relaxation.

(2) At a time 12 seconds into the deceleration cycle (fig. 6) the fourth layer is still in considerable tension. The top layer is also subject to tensile stresses now, though these are predicted not to exceed the modulus of rupture.

(3) At idle conditions (fig. 7) the top layer of the seal is once again predicted to be heavily in compression.

The performance of the zirconia/CoCrAlY layers would be expected to be far better under compression than when in tension. Thus a conclusion from the aforementioned results might be that apart from the rather high tensile stresses in the 40/60 zirconia/CoCrAlY layer, the possibility of the seal remaining structurally intact during thermal cycling appears to be reasonable. This is not entirely in accord with experimental evidence from thermal fatigue testing where surface cracks have developed. However, it must be recalled that it has been assumed that the seal is in a stress-free state at ambient conditions. Its method of manufacture is such as to suggest that residual tensile stresses might be present in the surface layer. Experimental determination of the residual stress distribution (ref. 2) has indicated that the tensile stress near the seal surface at ambient conditions is of the order 20.7 MN/m^2 (3000 psi). If tensile stresses of this order of magnitude are superimposed on those predicted in the top layer of the seal at a time 12 seconds into the deceleration cycle (fig. 6), it can be seen that the modulus of rupture is exceeded. Indeed the analytical predictions begin to bear reasonable comparison with experimental evidence. The latter has shown surface cracking, proceeding radially and driven by the circumferential tensile stresses, but not catastrophic structural failure.

Figures 8, 9, and 10 show stress distributions calculated by two-dimensional analyses for the same conditions as figures 5, 6, and 7, respectively. The results are presented primarily for comparison with the three-dimensional cases and to assist in realistic interpretation of the results of future two-dimensional analyses should they prove appropriate. It is apparent that the trends of the calculated stresses of figures 8, 9, and 10 bear comparison with the three-dimensional analysis results. It is also particularly noticeable that at a time 12 seconds into the deceleration cycle, the two-dimensional analyses predict greater tensile stresses in the surface layer.

The results presented thus far have been for a seal subject to the gas temperature cycle of figure 2 and heat-transfer coefficients of 5700 and 11 400 $W/(m^2)(K)$ (1000 and 2000 $Btu/(hr)(ft^2)(^oF)$) at the seal surface and back face, respectively. Brief consideration will be given here to the effect on stress patterns of two modifications to these conditions.

(1) Alternative Boundary Heat-Transfer Coefficients

In figure 4, the effect on the tempera. re distribution through the seal of two alternate combinations of boundary heat-transfer coefficients to those employed in obtaining the data of figure 3 have been presented. Two-dimensional finite-element computer program calculations have indicated that the difference in temperature distributions would cause relatively small differences in stress patterns. An examination of figure 4 adds weight to this conclusion, particularly when it is observed that the temperature distributions at 12 seconds into the deceleration cycle and at idle conditions do not vary much. Indeed, the most obvious effect on the stress distributions was predicted at steady-state sea-level take-off conditions; the circumferential stresses in the top ceramic layer near the interface with the second layer were somewhat more tensile for case 2 of figure 4 - heat-transfer coefficients of 570 $W/(m^2)(K)$ (100 $Btu/(hr)(ft^2)(^oF)$) and 11 400 $W/(m^2)(K)$ (2000 $Btu/(hr)(ft^2)(^oF)$) at the surface and back face - than for the other two cases. It is concluded that the lack of good data as regards heat-transfer coefficients may not be a significant drawback in analytical attempts to improve the cyclic thermal stressing behavior of the seal.

(2) An Alternative Variation of Compressor Cooling-Air Temperature

The hot turbine gases and cooling compressor air were assumed to vary in temperature during the deceleration cycle as shown in figure 2. These variations were assessed from calculated engine seal segment temperature cycles (ref. 2). The seal specimens have, however, been subjected to a slightly different thermal cycle during fatigue testing (ref. 2). In particular, the temperature of the back face of the metallic substrate fell only to about 616 K (650^o F) at idle simulation, rather than the 449 K (350^o F) indicated in figure 2. It might be felt that such a difference could be significant, perhaps causing more pronounced maximizing of the seal temperature below the surface, and possibly more adverse stressing.

To investigate this it was assumed that the compressor cooling air temperature varied linearly from 894 K (1150^o F) to 616 K (650^o F) during the 60-second deceleration cycle. The hot turbine gases were maintained at the same temperatures during the cycle. Of course, at sea-level take-off steady conditions, the temperature and stress distributions are the same as

presented already. At 12 seconds into the deceleration cycle the temperature and stress profiles were calculated to be as shown in figure 11.

The surface and maximum seal temperatures were, respectively, 1010 K (1359° F) and 1084 K (1492° F), compared to 987 K (1317° F) and 1020 K (1377° F) for case C of figure 3. As can be seen by inspecting figure 11 and comparing the magnitude of stresses indicated in figure 6, significantly higher circumferential stresses are predicted in the top ceramic layer with the higher back face cooling air temperature. Once again, however, the predicted stress pattern is consistent with available thermal fatigue experimental evidence.

Relieving the Surface Tensile Stresses

Both experimental thermal cycling tests and the analyses presented here (of residual stresses are accounted for) suggest that undue tensile stresses occur on the top, 100 percent yttria stabilized zirconia, layer of the seal. Consideration has been given to two schemes whereby such tensile stresses could be reduced.

(1) Applying a Bending Moment to the Substrate Before Spraying the Ceramic Layers

If a bending moment were applied to the substrate such that the surface to which the ceramic coats were applied was in tension before spraying, then on release of the substrate from the bending moment after spraying the ceramic layers would tend to be compressed. A calculation has been performed to estimate the magnitude of such a compressive effect which would be superposed on other residual stresses present.

A bending moment of about 360 Nm/m width applied only to the metallic seal substrate in the circumferential plane would result in surface circumferential stresses of magnitude about equal to the modulus of rupture, 276 MN/m^2 (40 000 psi). Such a bending moment was considered applied to the substrate of the assembled seal tending to cause compression of the ceramic layers. This was intended to represent the stress behavior of the seal after the bending moment had been released.

In figure 12 the compressive circumferential stresses calculated to result in the surface layer are shown. The circumferential stresses in the

other layers are lower than in the top layer. As can be seen the compressive stresses near the surface are estimated to be about 13 MN/m^2 (1886 psi). Such a magnitude of stress is not insignificant compared to the circumferential surface stresses shown in figure 6, and might be thought of as going a long way to offset the measured surface residual tensile stress on manufacture. It should be noted that the stress state in the substrate which would result would not be greatly different from that with the bending moment applied to it alone during spraying.

(2) Annealing the Seal

A common means of reducing residual stresses in components is to subject them to an annealing process. That is a component is heated to a temperature at which creep occurs relieving internal stresses. With a part having a composite material structure, such as the outer gas path seal, if a stress-free state is so induced at an elevated temperature then at normal ambient temperature some stress distribution will result.

For calculation purposes only it was assumed that a stress-free state was induced in the gas path seal at a temperature of 1366 K (2000° F). The stress distribution in the seal at a temperature of 294 K (70° F) was then determined to be as shown in figure 13. It was assumed that all materials exhibited elastic behavior with properties linearly extrapolated, where required, from those presented in table I.

As can be seen from figure 13 very substantial compressive stresses are postulated in the ceramic layers. The calculations suggest that some measure of annealing would be a very powerful means to pre-compress the seal, however, control might be difficult.

CONCLUDING REMARKS

Numerical schemes enabling the solution of transient temperature distributions and thermal stress patterns in an aircraft gas turbine outer gas path seal have been outlined. Sample results have been presented. The suite of computer programs employed gives a flexible base from which to study the behavior of the seal in more detail.

Certain features of the analyses merit further attention.

(1) The aspect ratio of the finite elements used in the stress analyses. In particular, for the three-dimensional analysis, 20 node bricks were used, 42 elements in all being employed. A typical brick had an aspect ratio of 20:10:1. which is not unreasonable. However, the effect of a more refined mesh of bricks should be investigated.

(2) The detail of the stress variation at the seal edges. The analyses conducted have indicated that very high rates of change of stress can occur at the axial and circumferential extremities of the seal. Such rates of change have not been modeled very well and the effect could bear further attention.

In addition, in order to simplify the analysis of computer results, an effective stress required for material failure according to the most appropriate of the current criteria should be employed. As regards parametric studies to attempt to define an improved gas path seal geometry, the following merit consideration.

(1) A more precise determination of a representative axial variation in temperature of the seal.

(2) An optimization of relative layer depths in the seal. The results presented in this report indicate that the minimization of the tensile stress in the top ceramic layer would be a suitable criterion for the optimization process. Minimization of this parameter should not cause problems elsewhere as long as the substrate temperature is maintained at an appropriate level.

(3) A study of a realistic engine seal geometry. The larger size seal which will be used in practice may exhibit characteristics not predicted by analysis of the test size seal.

SUMMARY OF RESULTS

(1) Transient temperature distributions in the outer gas path seal show a maximum below the seal surface. This tends to cause tensile stresses in the top ceramic layer.

(2) The magnitude of the heat-transfer coefficients used in the analysis at the seal surfaces are not highly significant.

(3) Stress analysis of the seal using two-dimensional finite element programs predicts trends consistent with the three-dimensional analysis results.

(4) The magnitude of the thermal stresses determined, taking account of residual stresses known to be present, suggests that the top ceramic layer of the seal suffers tensile stresses which exceed the modulus of rupture.

(5) Application of a circumferential bending moment to the substrate sufficient to cause near yielding in tension at the surface onto which the ceramic layers are then sprayed, results on modest compression of the top ceramic layer on release of the applied moment. Annealing of the seal appears to be a more powerful means of pre-compressing the ceramic layers.

(6) In the calculation of shear distrubitions it has been assumed that the seal is free to distort without any restrictions. Computations have indicated that if this is not the case, the stressing of the seal materials would be substantially greater.

REFERENCES

1. Technical Proposal for Development of Improved High-Pressure Turbine Outer Gas Path Seal Component. Submitted to NASA Lewis Research Center, Cleveland, Ohio by Pratt and Whitney Aircraft, East Hartford, Connecticut. Ref. No. 76-6340, 2nd August, 1976.

2. Continued Development of Abradable Gas Path Seals. Final Report Draft on Contract NAS3-19759. Pratt and Whitney Aircraft, 21st February, 1977.

PROPERTY	YSZ		85/15. YSZ/CoCrAlY		70/30. YSZ/CoCrAlY		40/60. YSZ/CoCrAlY		MAR-M-509	
	TEMP K		TEMP. K		TEMP K		TEMP K		TEMP. K	
DENSITY (kg/m^3)	ALL	4290	ALL	4982	ALL	5674	ALL	7031	ALL	8858
POISSON'S RATIO	ALL	0.25	ALL	0.26	ALL	0.27	ALL	0.28	ALL	0.30
YOUNG'S MODULUS (GN/m^2)	294	46.9	294	25.4	294	36.2	294	58.6	700	197
	1589	15.6	1144	18.6	1061	47.0	1005	92.4	1144	155
MODULUS OF RUPTURE (MN/m^2)	294	28.2	294	41.4	294	56.3	294	223	700	276
	1589	22.9	1144	47.0	1061	70.3	1005	108	1144	276
COEFFICIENT OF EXPANSION ($K^{-1} \times 10^6$)	294	7.38	294	6.12	294	6.30	294	6.84	700	14.4
	1589	8.64	1144	11.0	1061	11.3	1005	12.2	1144	17.1
SPECIFIC HEAT ($J/kg\,K$)	476	550	476	534	476	516	476	483	476	445
	1366	646	1366	643	1366	638	1366	625	1366	609
THERMAL CONDUCTIVITY ($W/m\,K$)	366	0.51	366	0.51	366	0.51	366	0.51	366	15.0
	533	0.51	533	0.58	533	0.62	533	0.67	—	—
	811	0.54	811	0.78	811	0.93	811	1.04	—	—
	1089	0.59	1089	1.06	1089	1.32	1089	1.52	—	—
	1366	0.71	1366	1.45	1366	1.85	1366	2.20	—	—
	1644	1.01	1644	2.03	1644	2.61	1644	3.18	1644	52.7

YSZ = Y_2O_3 STABILIZED ZrO_2

MATERIAL PHYSICAL AND MECHANICAL PROPERTIES

TABLE 1

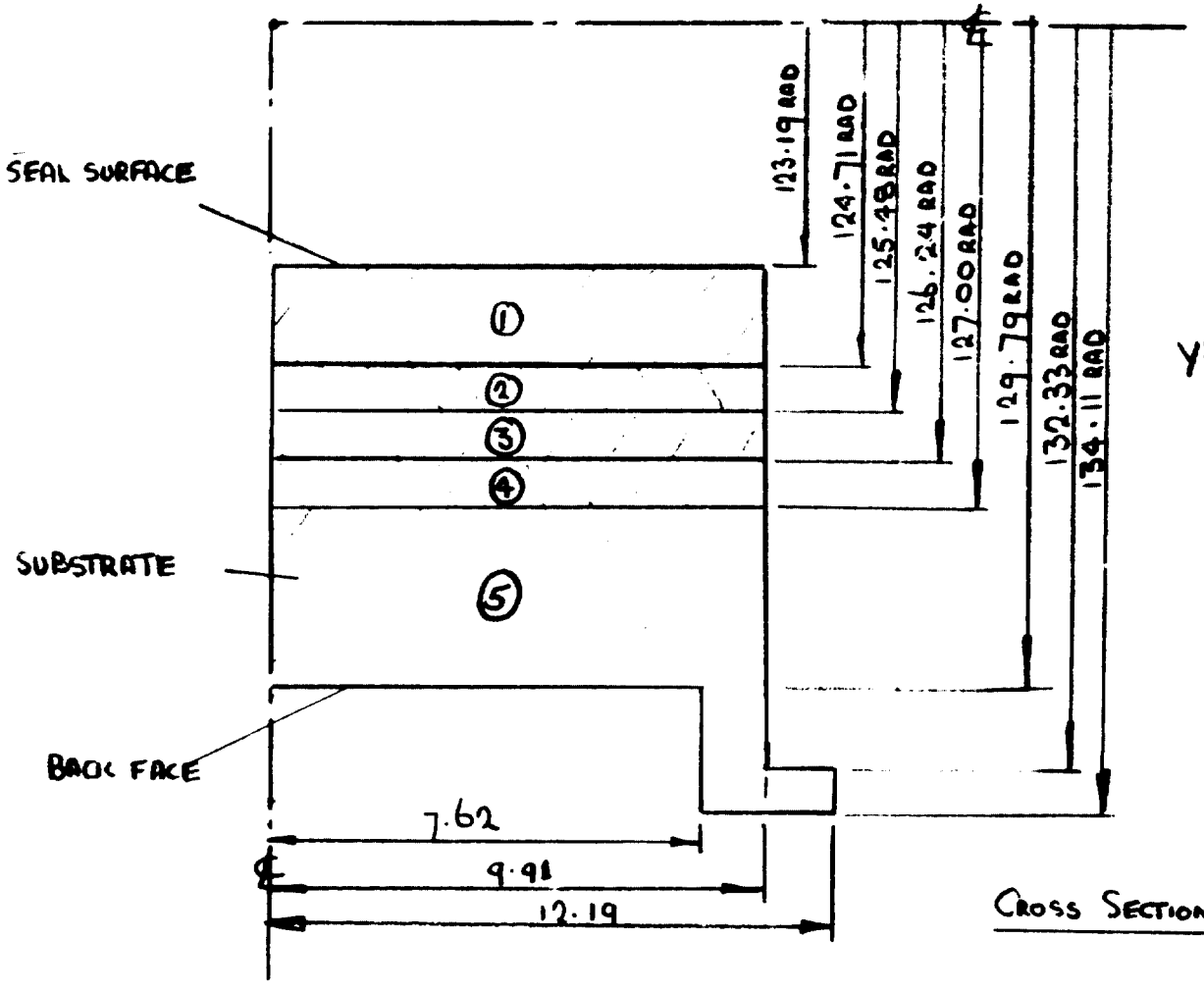

LAYER	MATERIAL (% BY WEIGHT)
①	100 YSZ
②	85/15 YSZ/CoCrALY
③	70/30 YSZ/CoCrALY
④	40/60 YSZ/CoCrALY
⑤	Mar-M-509

YSZ = Y_2O_3 STABILIZED ZrO_2

ANGULAR EXTENT OF SEAL = 0.559 rad.

CROSS SECTION OF OUTER GAS PATH SEAL (UNITS mm)

FIGURE 1

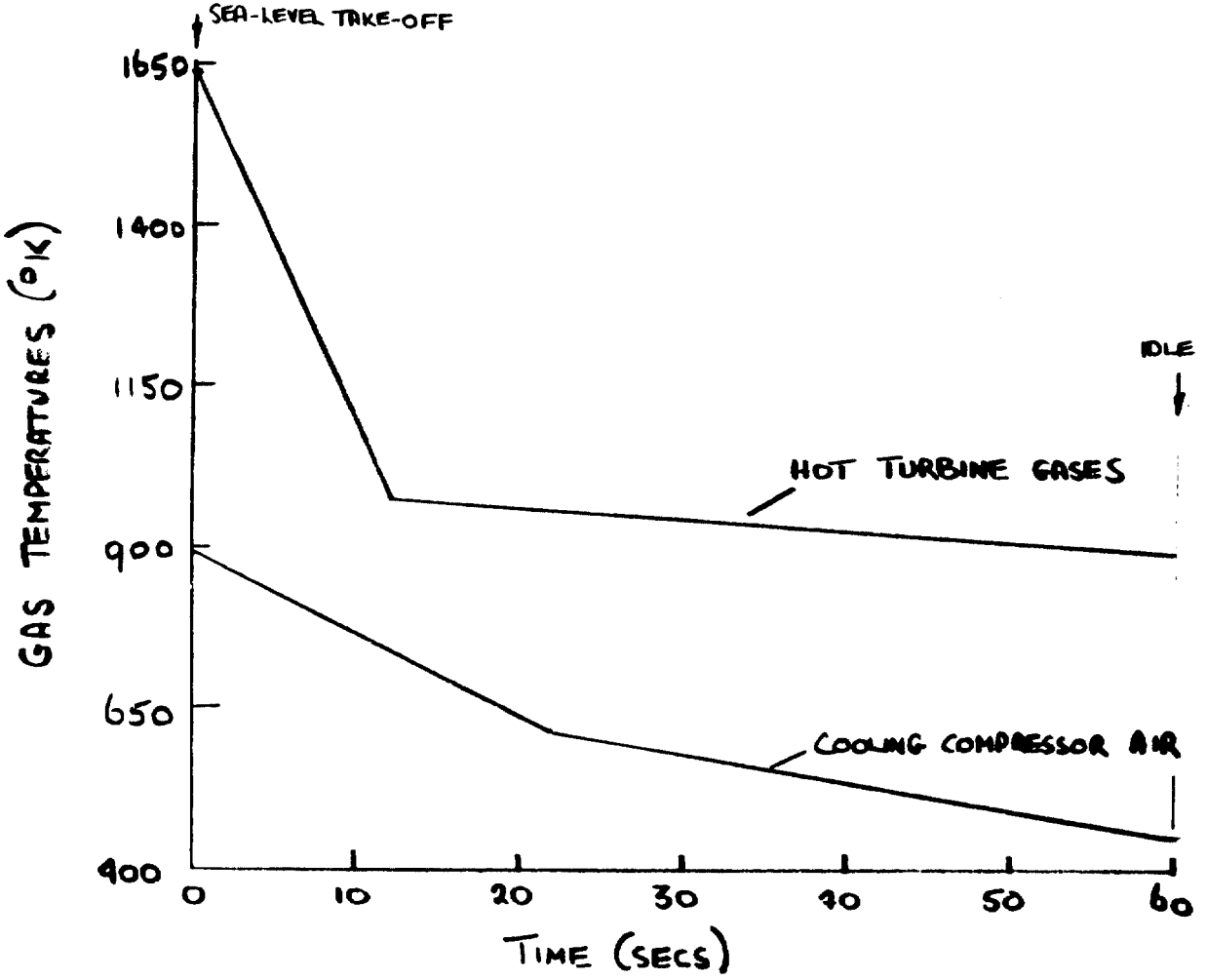

ASSUMED GAS TEMPERATURE VARIATIONS FROM SEA-LEVEL TAKE-OFF TO IDLE CONDITION

FIGURE 2

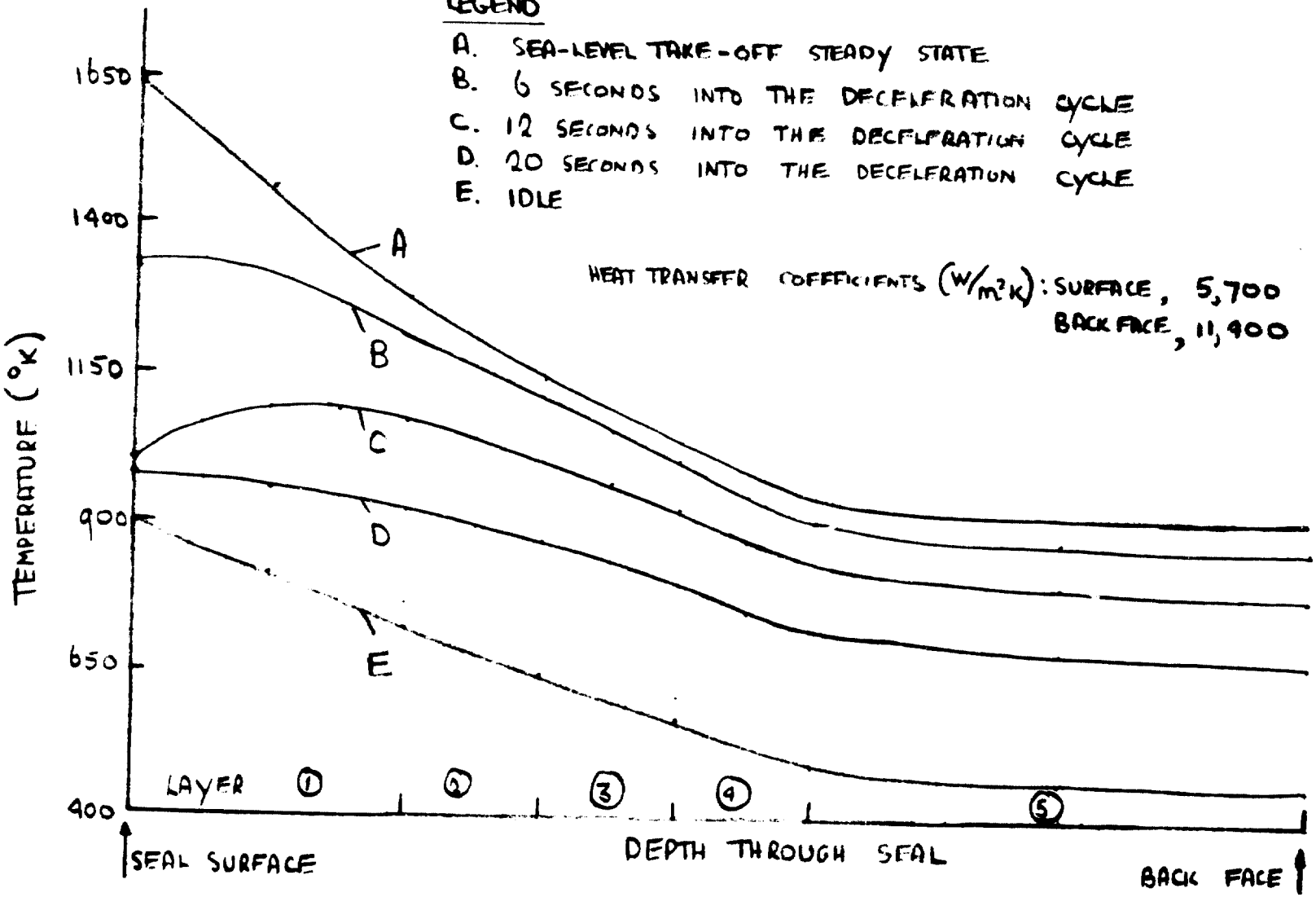

TRANSIENT TEMPERATURE PROFILES THROUGH THE SEAL ON THE AXIAL LINE OF SYMMETRY

FIGURE 3

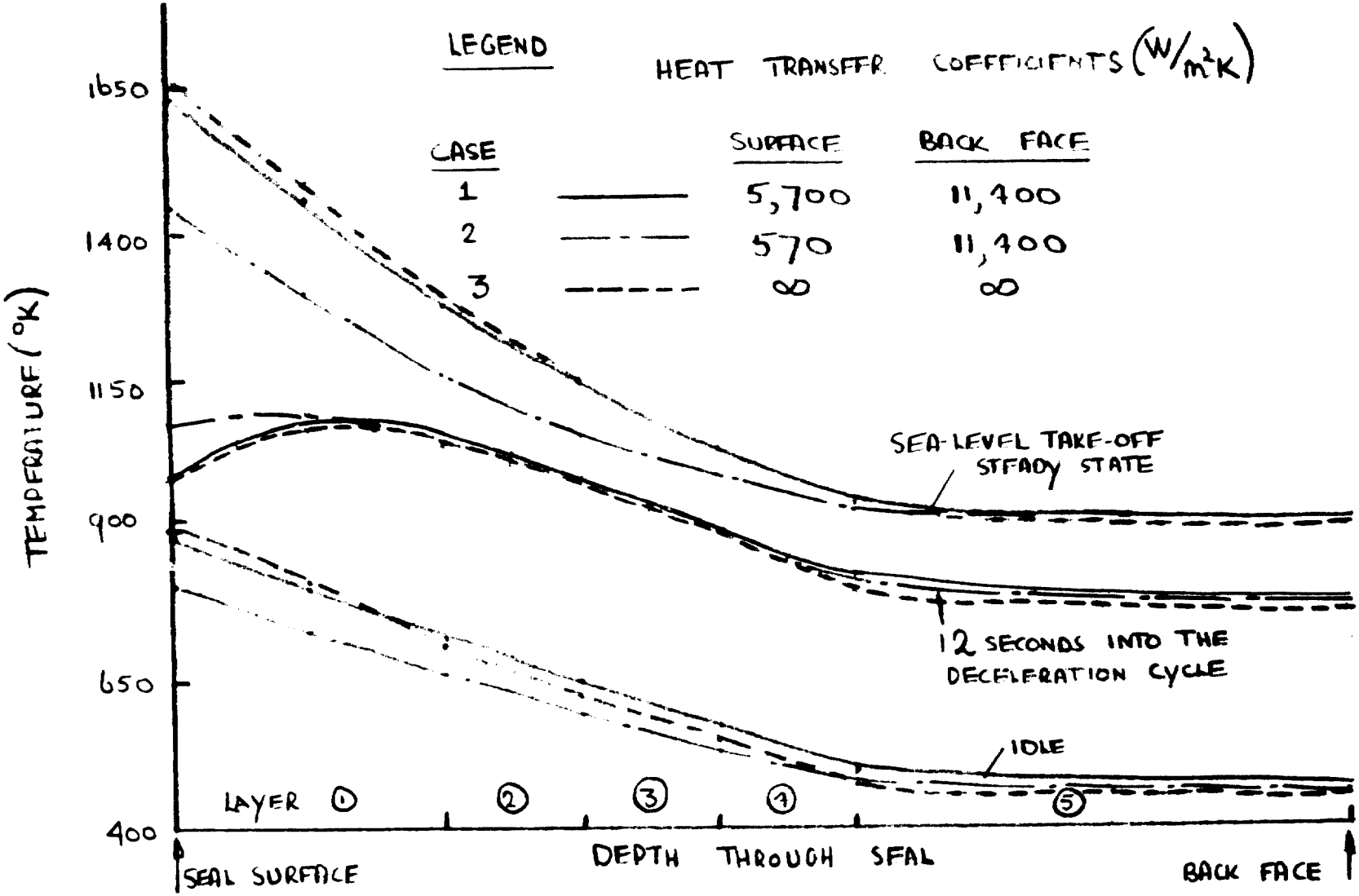

TEMPERATURE PROFILES THROUGH THE SEAL ON THE AXIAL LINE OF SYMMETRY FOR VARYING HEAT TRANSFER COEFFICIENTS

FIGURE 4

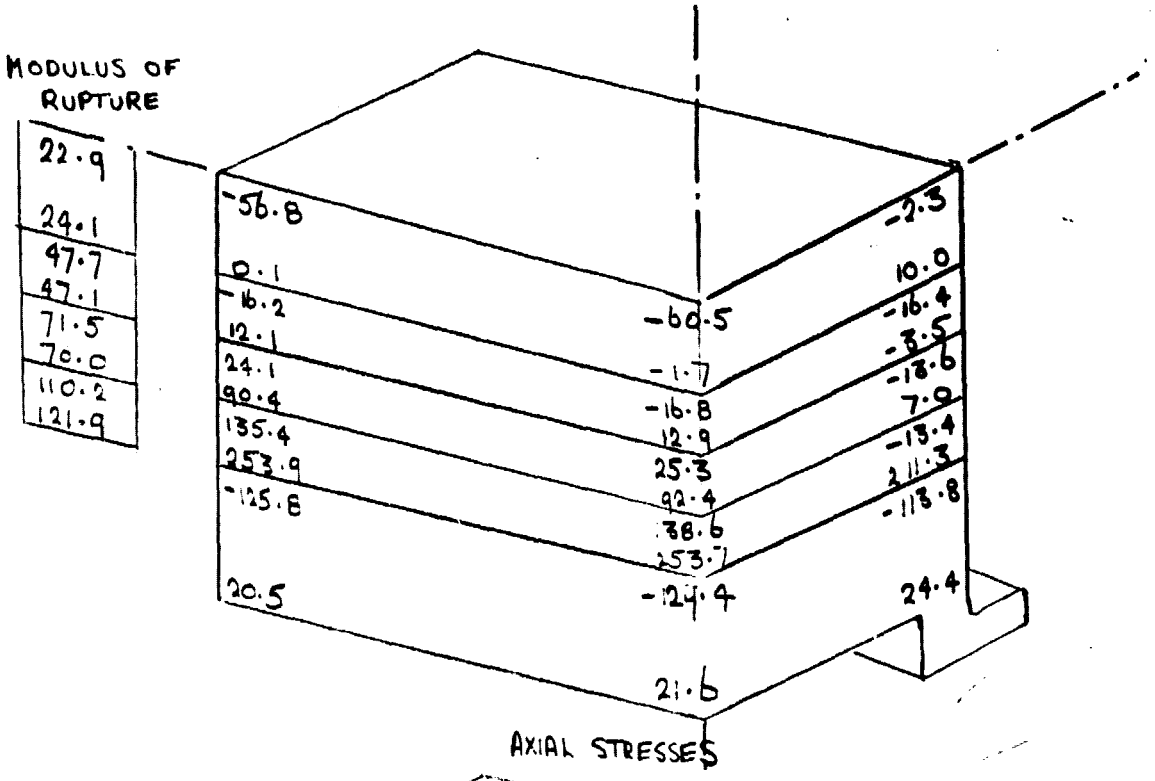

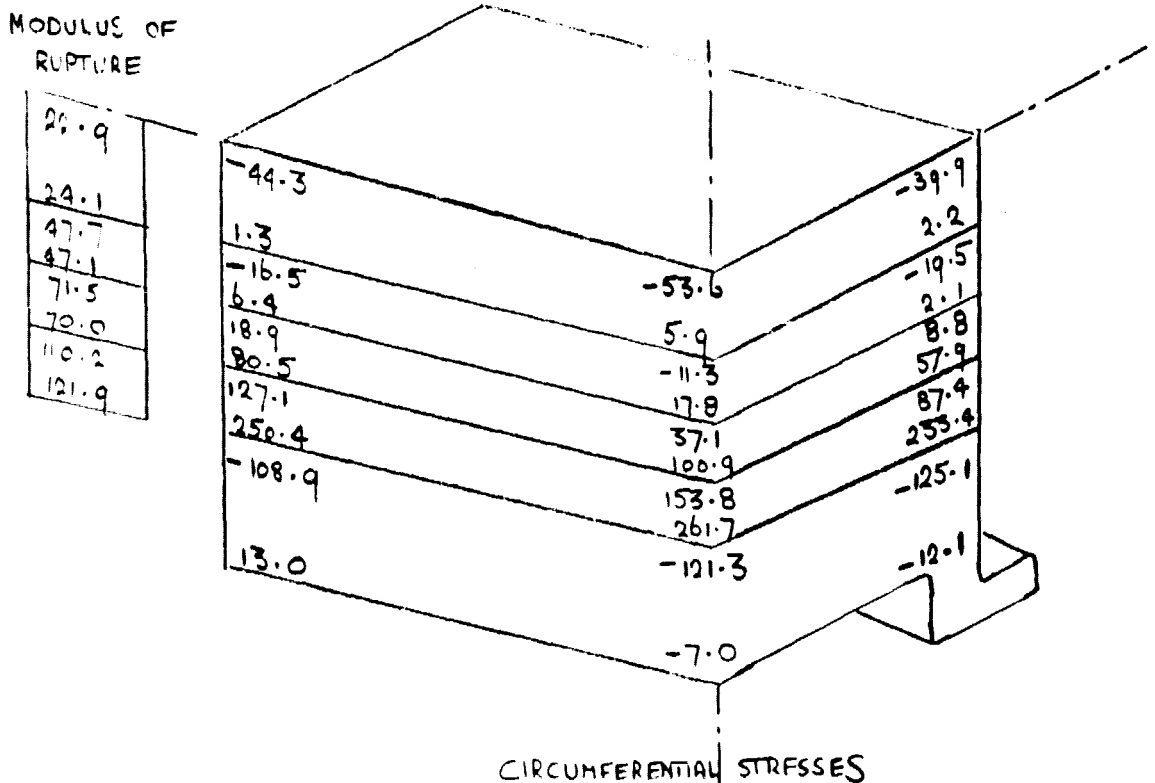

AXIAL AND CIRCUMFERENTIAL STRESSES IN OUTER GAS PATH SEAL.
SEA-LEVEL TAKE-OFF STEADY STATE (THREE DIMENSIONAL ANALYSIS. UNITS MN/m^2. TENSILE +ve)

FIGURE 5

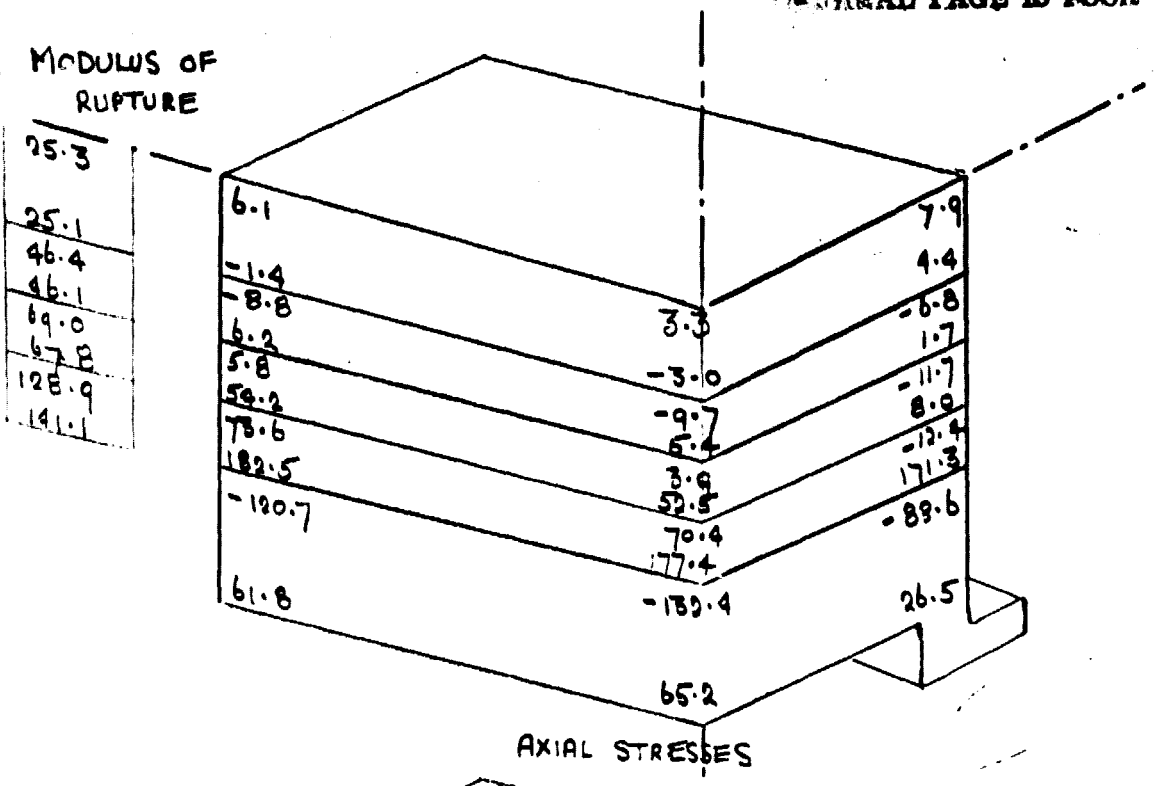

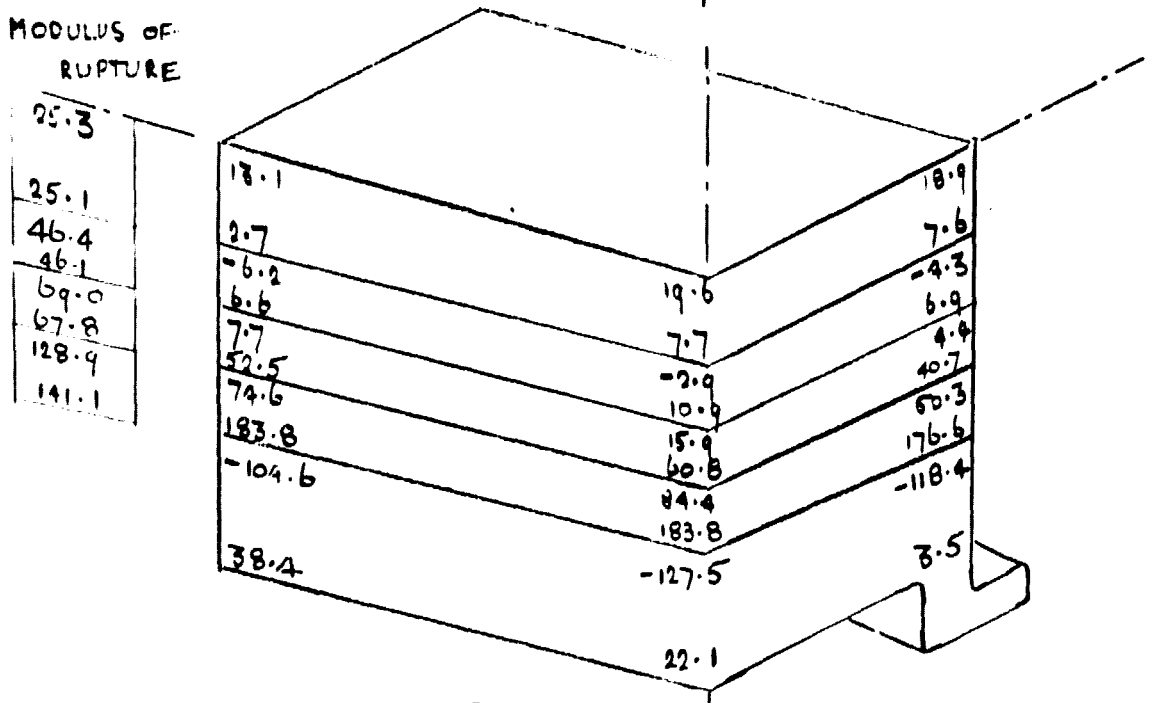

AXIAL AND CIRCUMFERENTIAL STRESSES IN OUTER GAS PATH SEAL.
12 SECONDS INTO THE DECELERATION CYCLE (THREE DIMENSIONAL ANALYSIS. UNITS MN/m^2
TENSILE +ve)

FIGURE 6

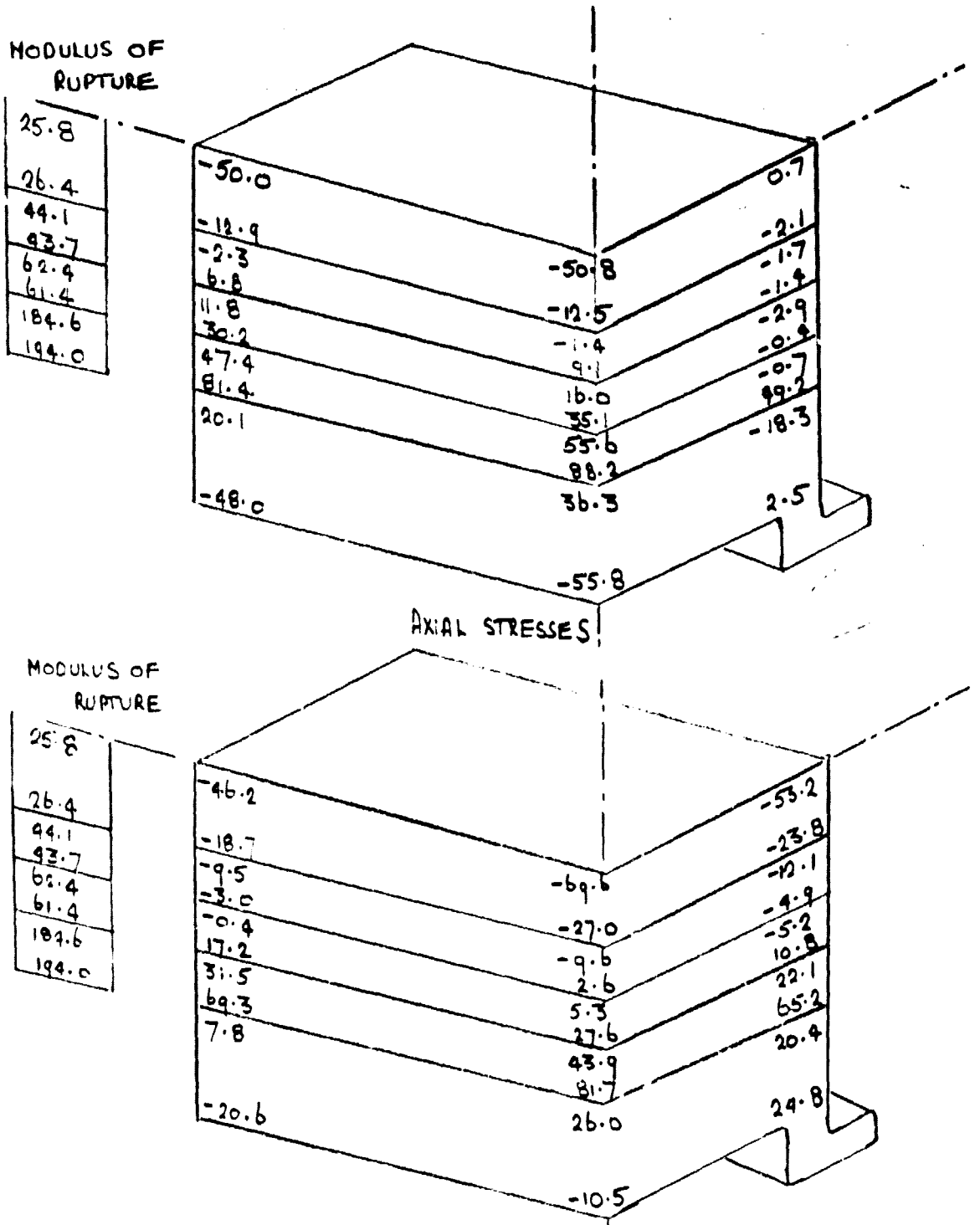

AXIAL AND CIRCUMFERENTIAL STRESSES IN OUTER GAS PATH SEAL. IDLE. (THREE DIMENSIONAL ANALYSIS UNITS MN/m^2. TENSILE +ve)

FIGURE 7

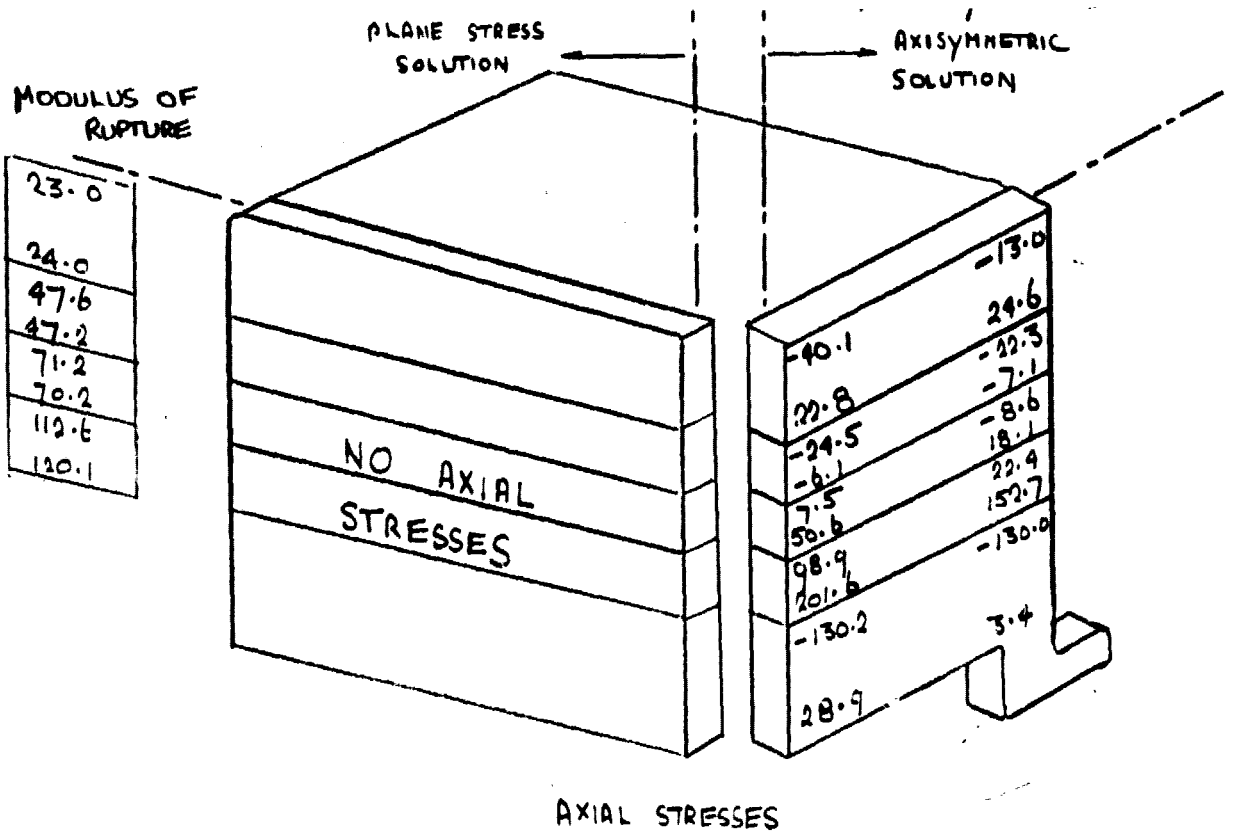

AXIAL STRESSES

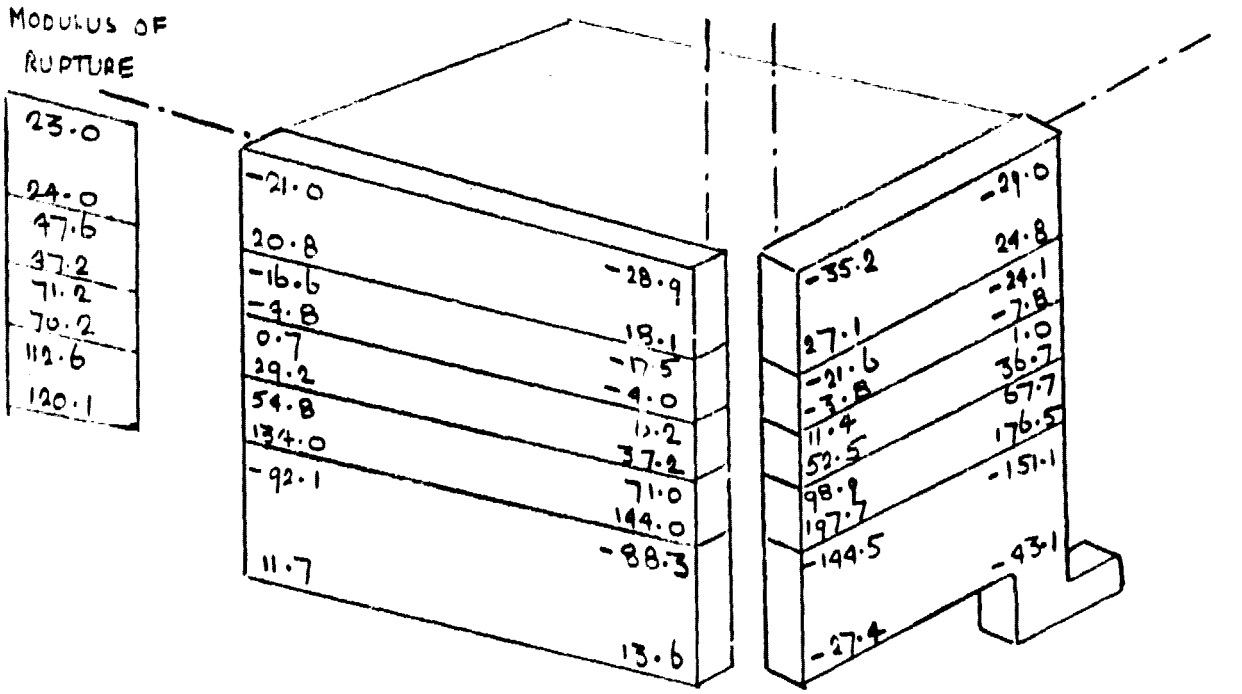

CIRCUMFERENTIAL STRESSES

AXIAL AND CIRCUMFERENTIAL STRESSES IN OUTER GAS PATH SEAL. SEA-LEVEL TAKE-OFF STEADY STATE (TWO DIMENSIONAL ANALYSES. UNITS MN/m^2. TENSILE +ve)

FIGURE 8

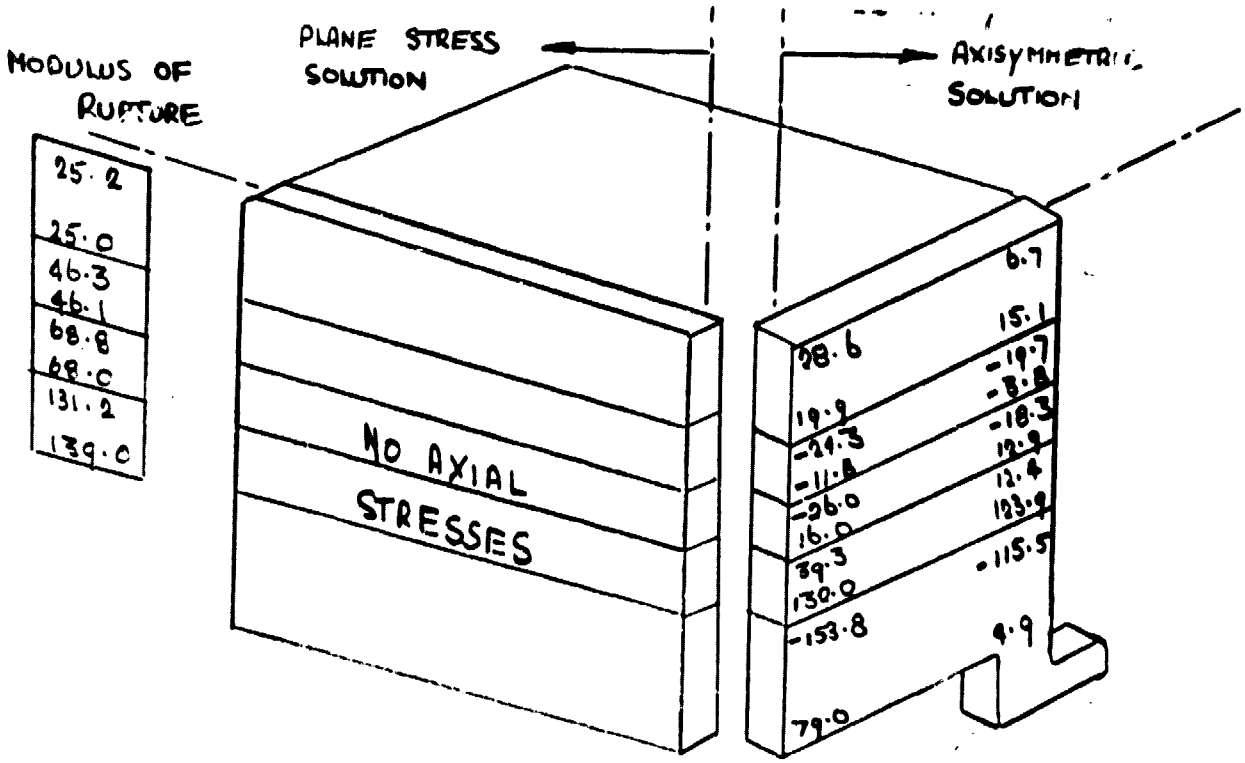

AXIAL STRESSES

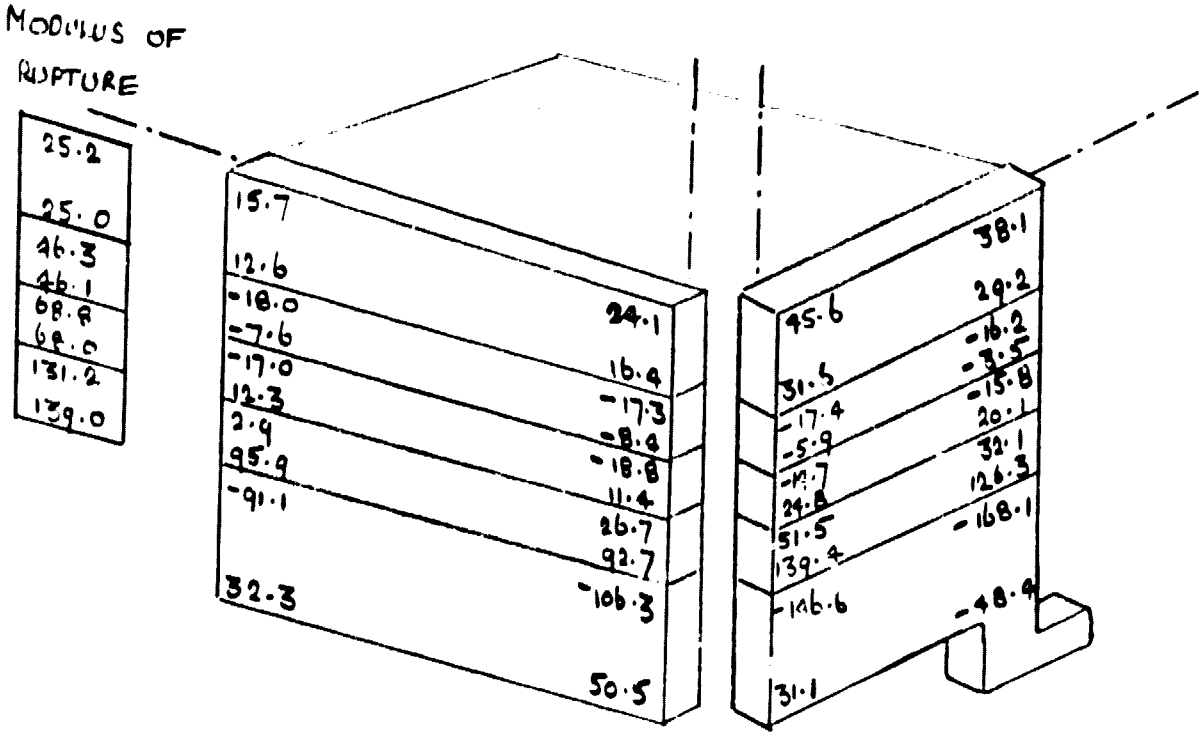

CIRCUMFERENTIAL STRESSES

AXIAL AND CIRCUMFERENTIAL STRESSES IN OUTER GAS PATH SEAL. 12 SECONDS INTO THE DECELERATION CYCLE (TWO DIMENSIONAL ANALYSES. UNITS MN/m^2. TENSILE +VE)

FIGURE 9

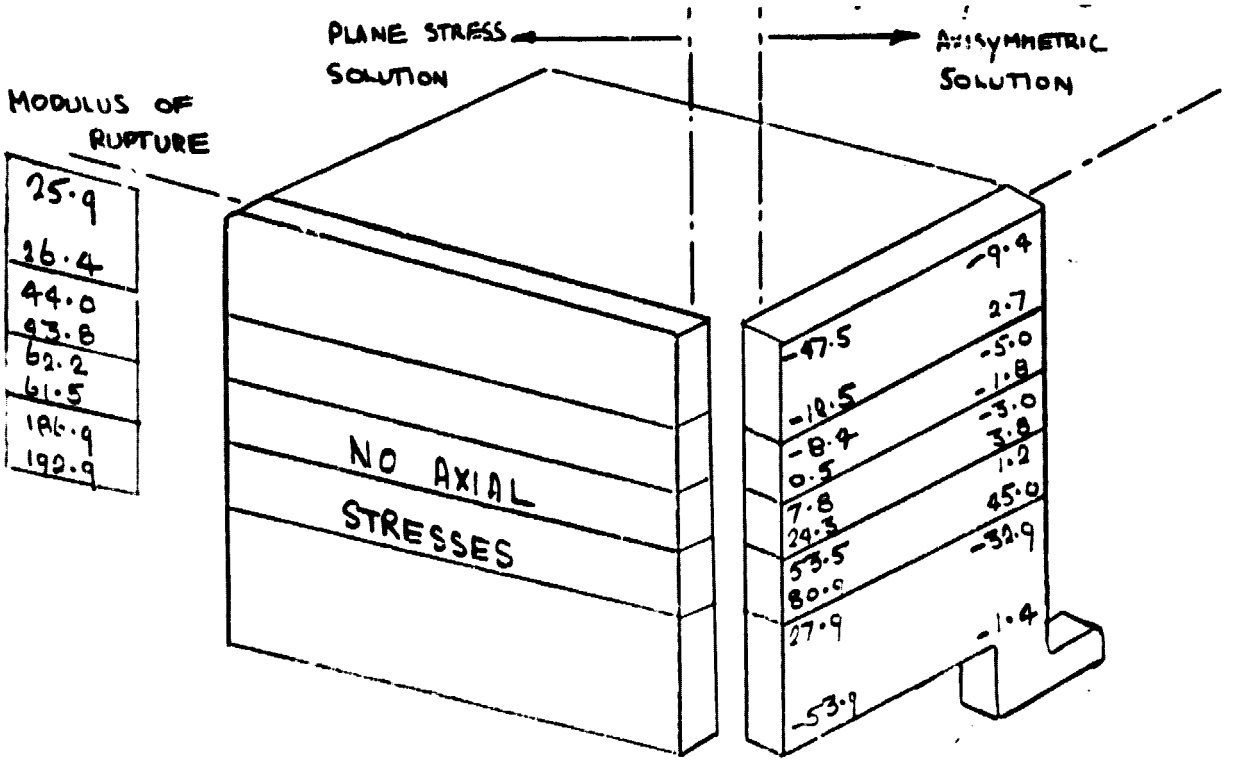

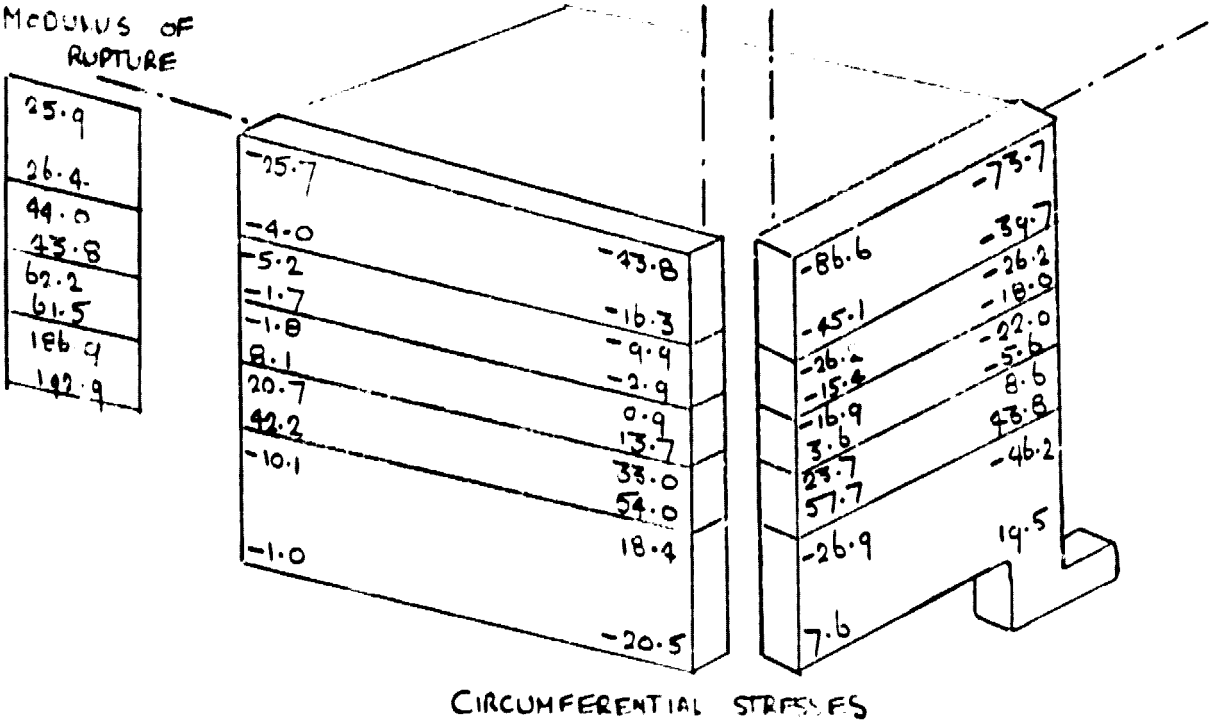

AXIAL AND CIRCUMFERENTIAL STRESSES IN OUTER GAS PATH SEAL. IDLE (TWO DIMENSIONAL ANALYSES. UNITS MN/m². TENSILE +ve)

FIGURE 10

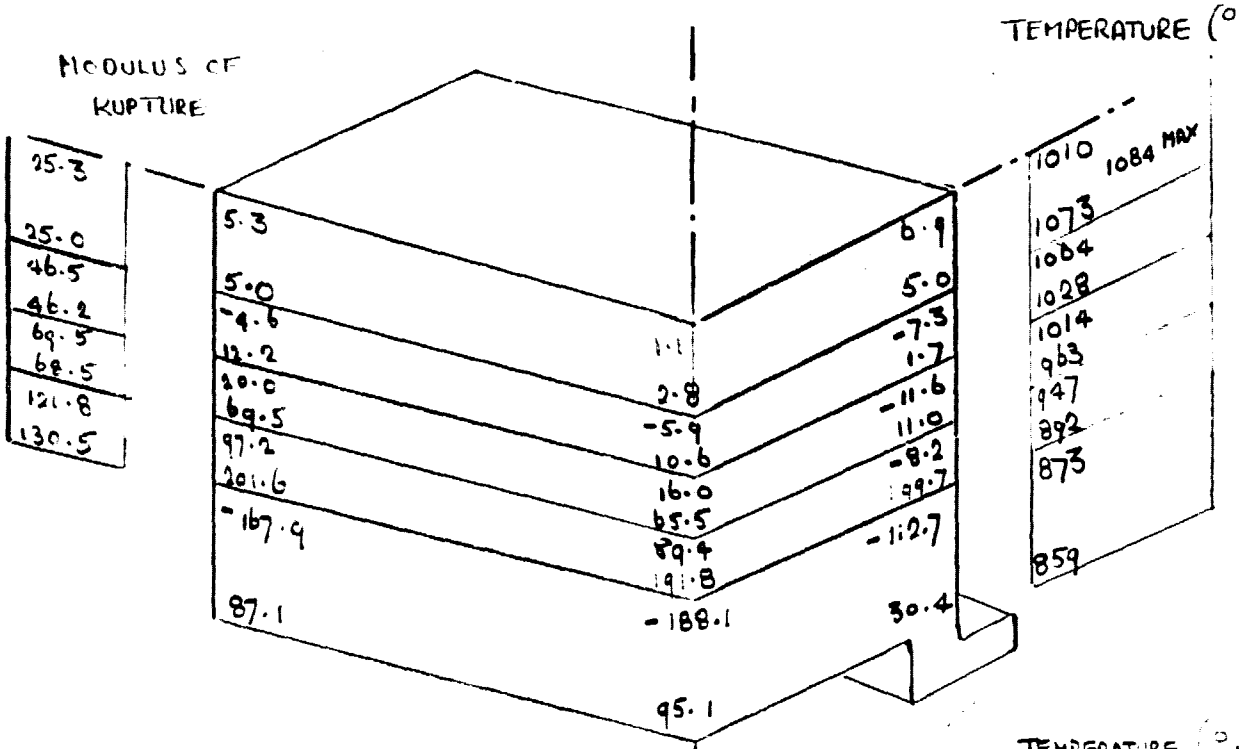

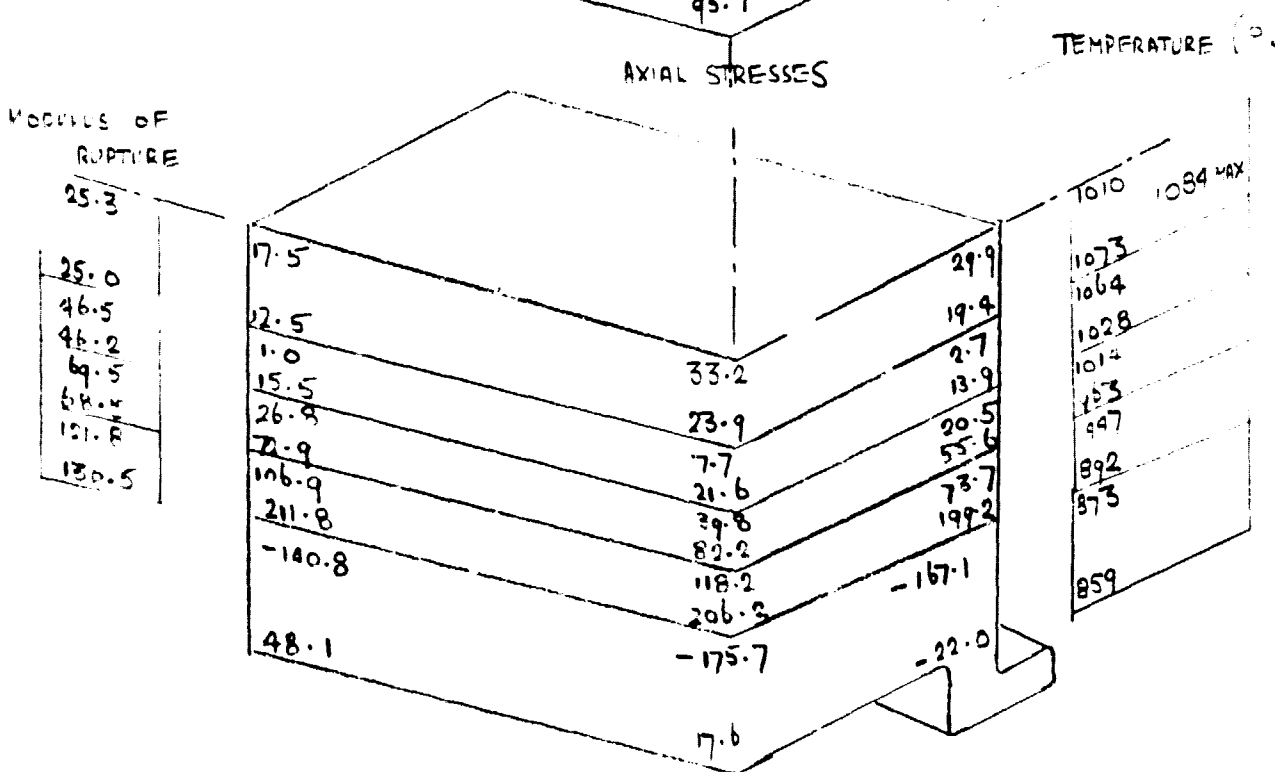

CIRCUMFERENTIAL STRESSES

AXIAL AND CIRCUMFERENTIAL STRESSES IN OUTER GAS PATH SEAL WITH ALTERNATIVE COMPRESSOR COOLING AIR TEMPERATURE, 12 SECONDS INTO THE DECELERATION CYCLE. (THREE DIMENSIONAL ANALYSIS. UNITS MN/m^2, TENSILE +VE)

FIGURE 11

FIGURE 12

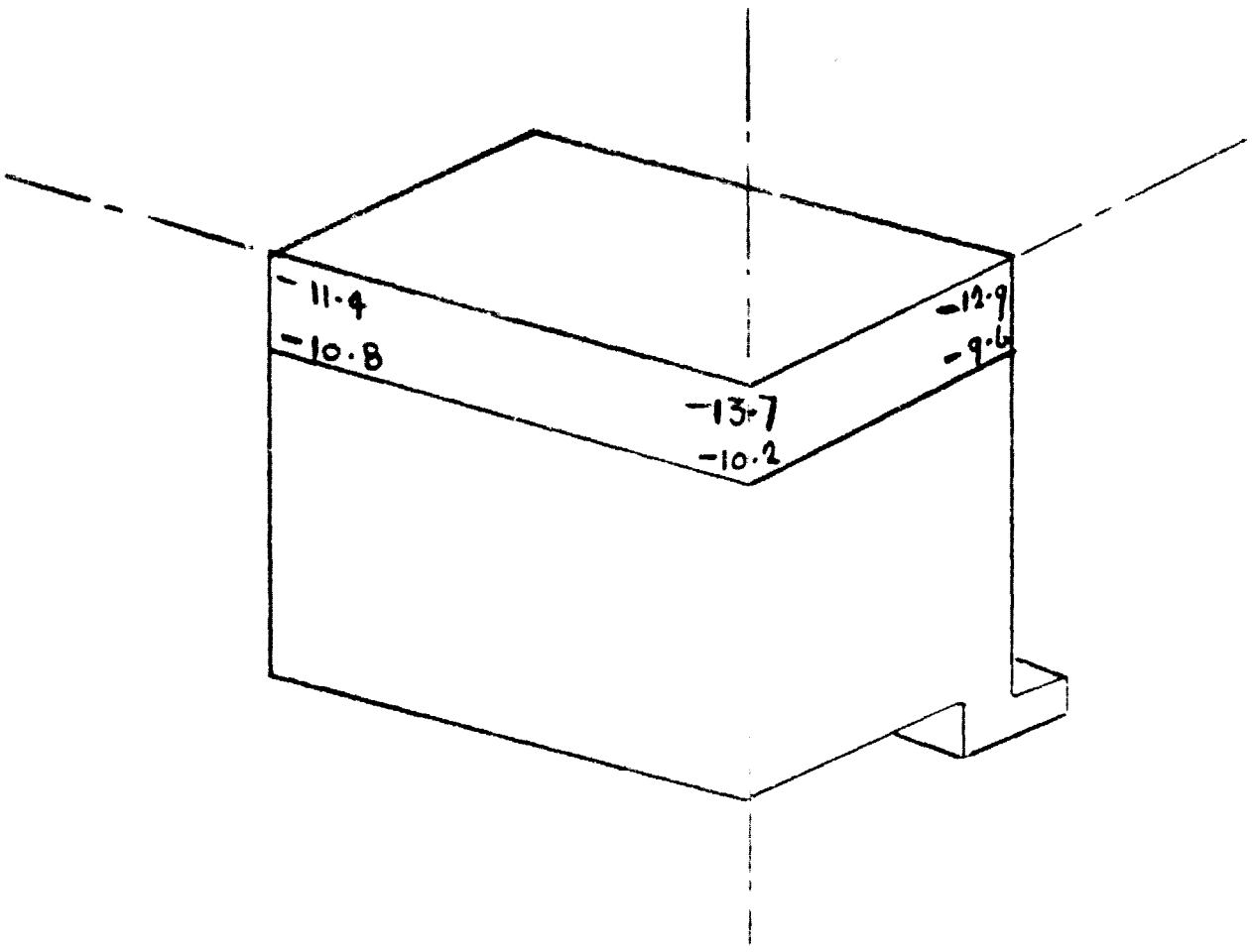

CIRCUMFERENTIAL STRESSES

COMPRESSIVE STRESS DEVELOPED IN THE SURFACE LAYER DUE TO APPLYING BENDING MOMENT OF 360Nm/METRE WIDTH TO THE SUBSTRATE IN THE CIRCUMFERENTIAL PLANE (UNITS MN/m^2)

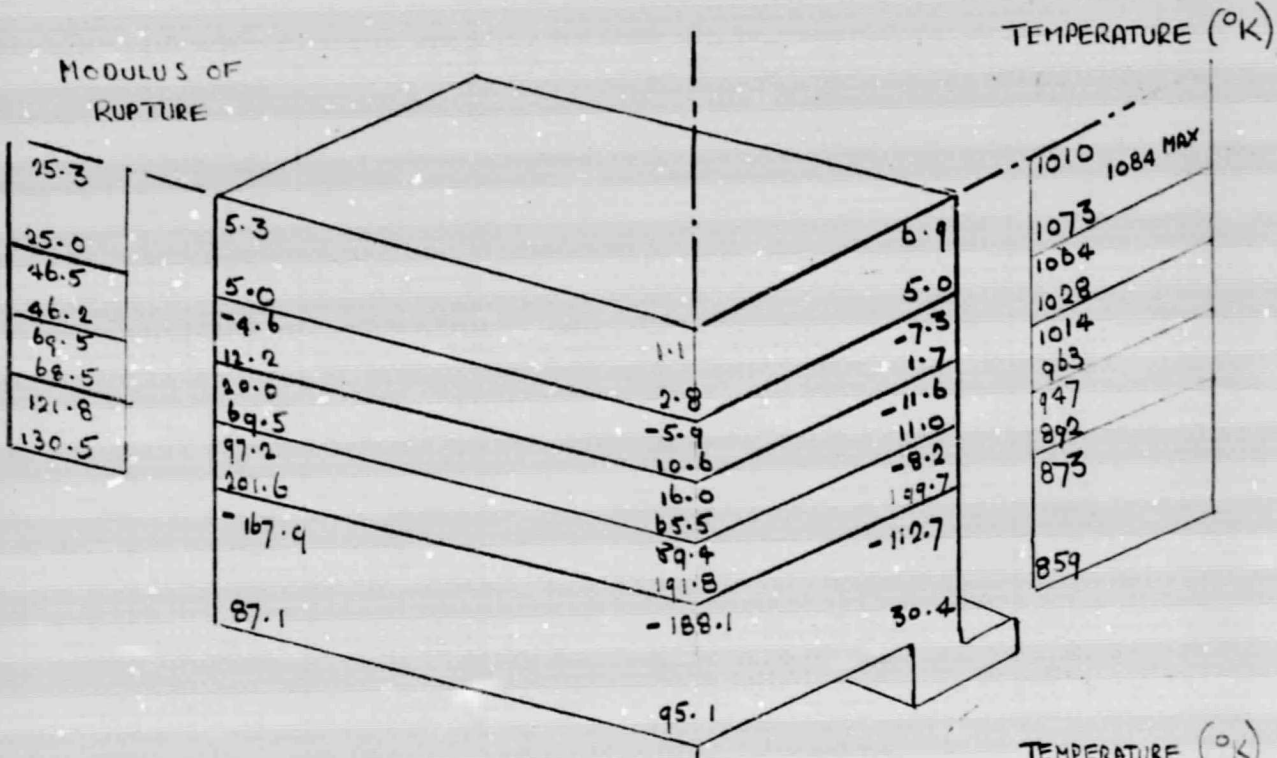

AXIAL AND CIRCUMFERENTIAL STRESSES IN OUTER GAS PATH SEAL WITH ALTERNATIVE COMPRESSOR COOLING AIR TEMPERATURE, 12 SECONDS INTO THE DECELERATION CYCLE. (THREE DIMENSIONAL ANALYSIS. UNITS MN/m^2. TENSILE +ve)

FIGURE 11

FIGURE 12

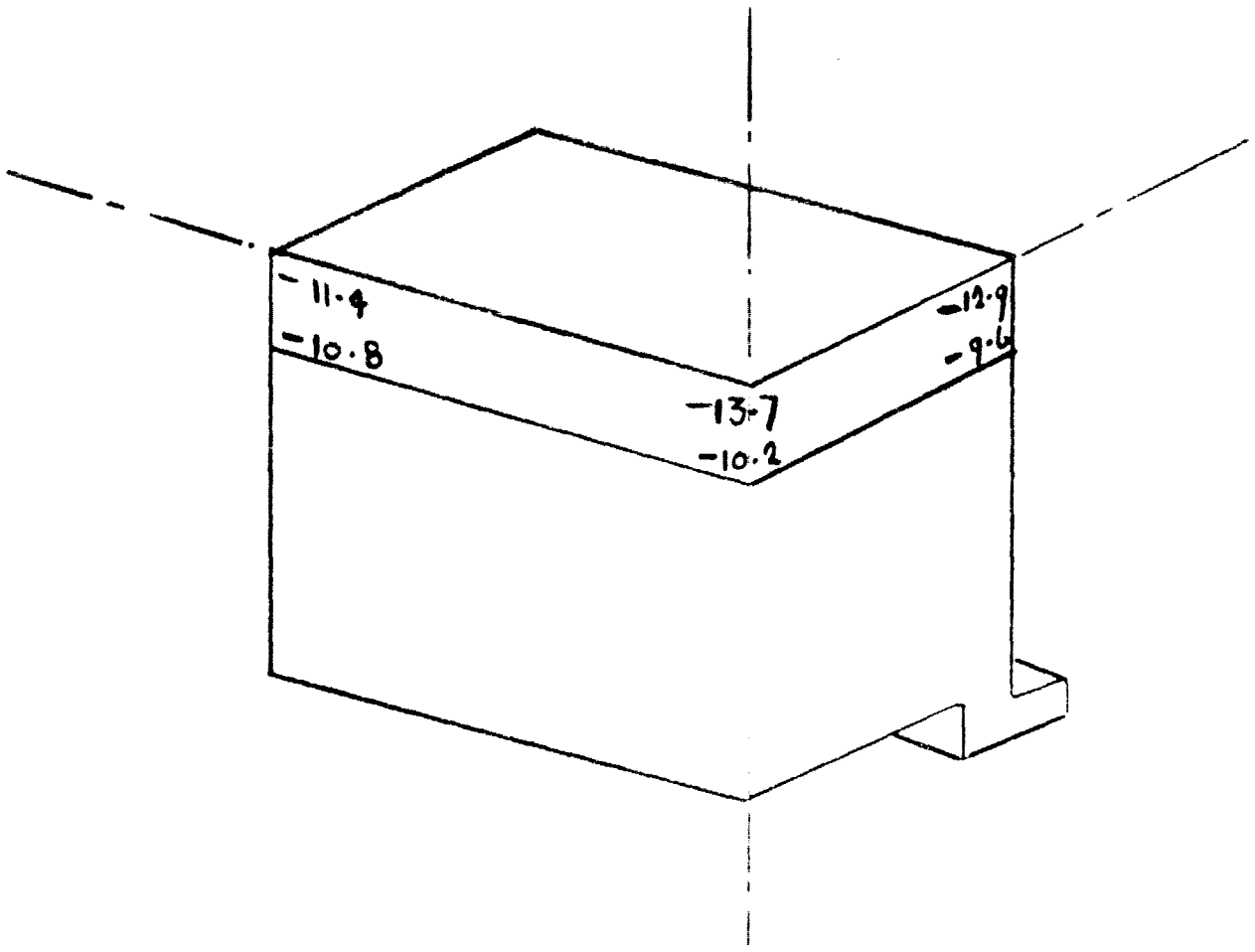

CIRCUMFERENTIAL STRESSES

COMPRESSIVE STRESS DEVELOPED IN THE SURFACE LAYER DUE TO APPLYING BENDING MOMENT OF 360Nm/METRE WIDTH TO THE SUBSTRATE IN THE CIRCUMFERENTIAL PLANE (UNITS MN/m^2)

FIGURE 12

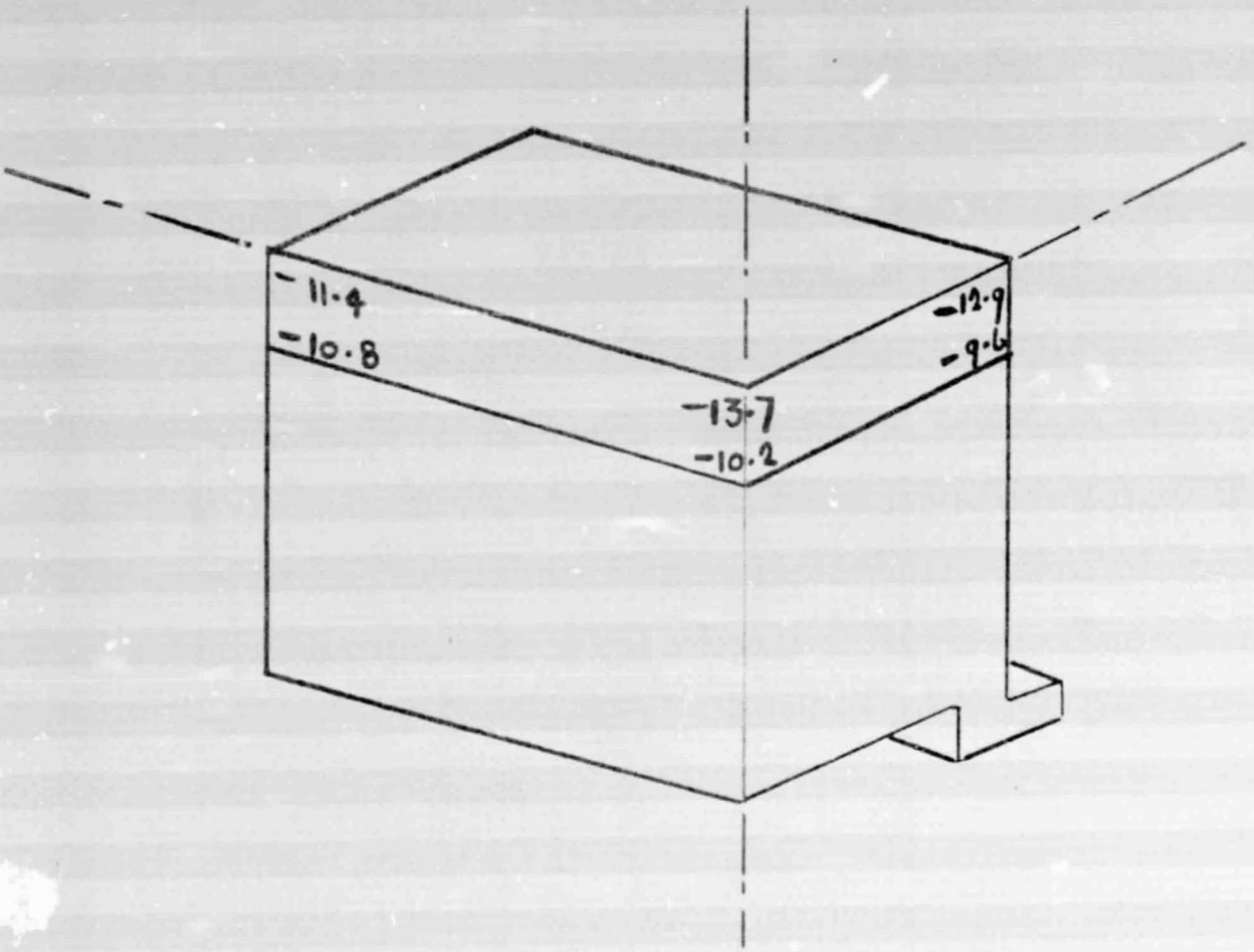

CIRCUMFERENTIAL STRESSES

COMPRESSIVE STRESSES DEVELOPED IN THE SURFACE LAYER DUE TO APPLYING BENDING MOMENT OF 360Nm/METRE WIDTH TO THE SUBSTRATE IN THE CIRCUMFERENTIAL PLANE (UNITS MN/m^2)